

**Supplemental Information**

**Dual Role of the Adaptive Immune System in Liver**

**Injury and Hepatocellular Carcinoma Development**

**Jessica Endig, Laura Elisa Buitrago-Molina, Silke Marhenke, Florian Reisinger, Anna Saborowski, Jutta Schütt, Florian Limbourg, Christian Könecke, Alina Schreder, Alina Michael, Ana Clara Misslitz, Marc Eammonn Healy, Robert Geffers, Thomas Clavel, Dirk Haller, Kristian Unger, Milton Finegold, Achim Weber, Michael P. Manns, Thomas Longerich, Mathias Heikenwälder, and Arndt Vogel**

## Supplemental Data

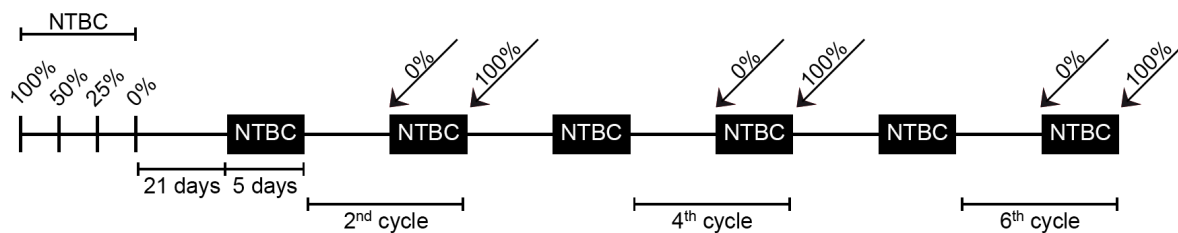


**Figure S1, related to Figure 1: Schedule of NTBC cycling**

NTBC content in the drinking water was gradually reduced over three days and mice were kept off NTBC for 21 days, followed by a five-day period on 100% NTBC supplementation (black boxes). Mice were euthanized and livers were harvested after two, four and six courses of NTBC withdrawal and re-supplementation.

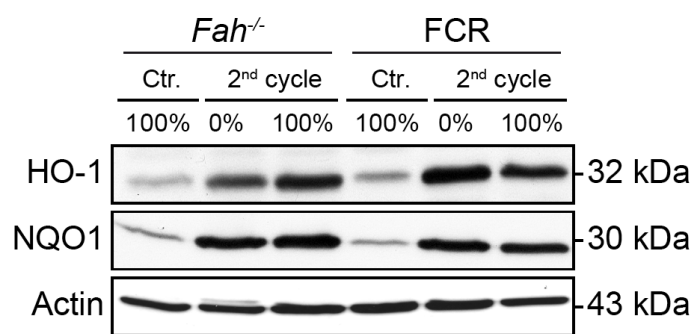


**Figure S2, related to Figure 2: FAA-induced liver damage leads to a strong activation of the Nrf2 pathway**

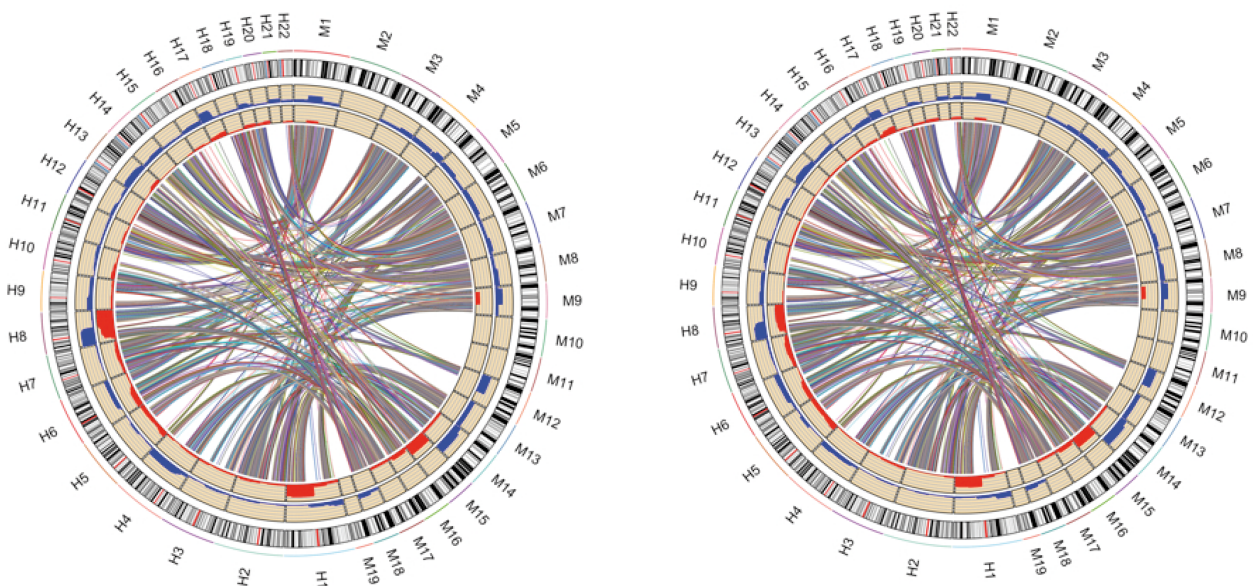
*Fah*<sup>-/-</sup> and FCR mice were cycled two times (0%) or kept on 100% NTBC. HO-1, NQO1 and Actin protein level was detected in liver homogenates via Western blotting. A strong induction of both proteins was evident in *Fah*<sup>-/-</sup> and FCR mice during NTBC cycling.

**Table S1, related to Figure 5:**

Provided as an Excel file.

**Table S2, related to Figure 5:**

<b>Viral</b>	<b>CNA</b>	<b>Number of</b>	<b>Human match</b>	<b>p-value</b>
	losses	7577	59.6	0,0002
	gains	1700	75.5	< 0.0001
<b>Hepatitis B</b>	<b>CNA</b>	<b>Number of</b>	<b>Human match</b>	<b>p-value</b>
	losses	7577	49.9	< 0.0001
	gains	1700	63.8	< 0.0001
<b>Hepatitis C</b>	<b>CNA</b>	<b>Number of</b>	<b>Human match</b>	<b>p-value</b>
	losses	7577	69.6	0.0024
	gains	1700	45.1	< 0.0001
<b>Alcohol</b>	<b>CNA</b>	<b>Number of</b>	<b>Human match</b>	<b>p-value</b>
	losses	7577	79.1	< 0.0001
	gains	1700	70.6	< 0.0001
<b>MYC</b>	<b>CNA</b>	<b>Number of</b>	<b>Human match</b>	<b>p-value</b>
	losses	7577	79.5	0.0001
	gains	1700	75.7	< 0.0001

**A** Comparison with *MYC*-induced HCC**B** Comparison with Alcohol-induced HCC**Table S1, S2 and Figure S3, related to Figure 5: Synteny analyses of genomic alterations in *Fah*<sup>-/-</sup> and human HCCs**

The frequencies of copy number alterations of the mouse model and the appropriate syntenic regions of the human TCGA HCC subset are visualized in Table S1, S2 and Figures S3. The best overlap between copy number alterations that were determined in our mouse model was observed with the alcohol and *MYC* induced alterations in the human HCC subgroups (overlap gains/ losses alcohol-derived: 70.6%/ 79.1% and *MYC*-alteration-derived: 75.7%/ 79.5%; p-values for all comparisons was  $\leq 0.0001$ ). The overlap with virus-derived HCC was smaller (hepatitis B-derived, gains/ losses: 63.8%/ 49.9% and hepatitis C-derived: 45.1%/ 69.6%; all p-values  $\leq 0.0001$  except that for losses in hepatitis C-derived cases which was 0.0024).

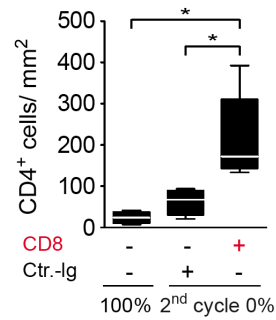


**Figure S4, related to Figure 7:** Quantification of CD4<sup>+</sup> T cells by IHC analysis. Intrahepatic CD4<sup>+</sup> T cells were significantly increased in cycled *Fah*<sup>-/-</sup> mice under CD8<sup>+</sup> cell depletion. Data are represented as mean  $\pm$  SD.

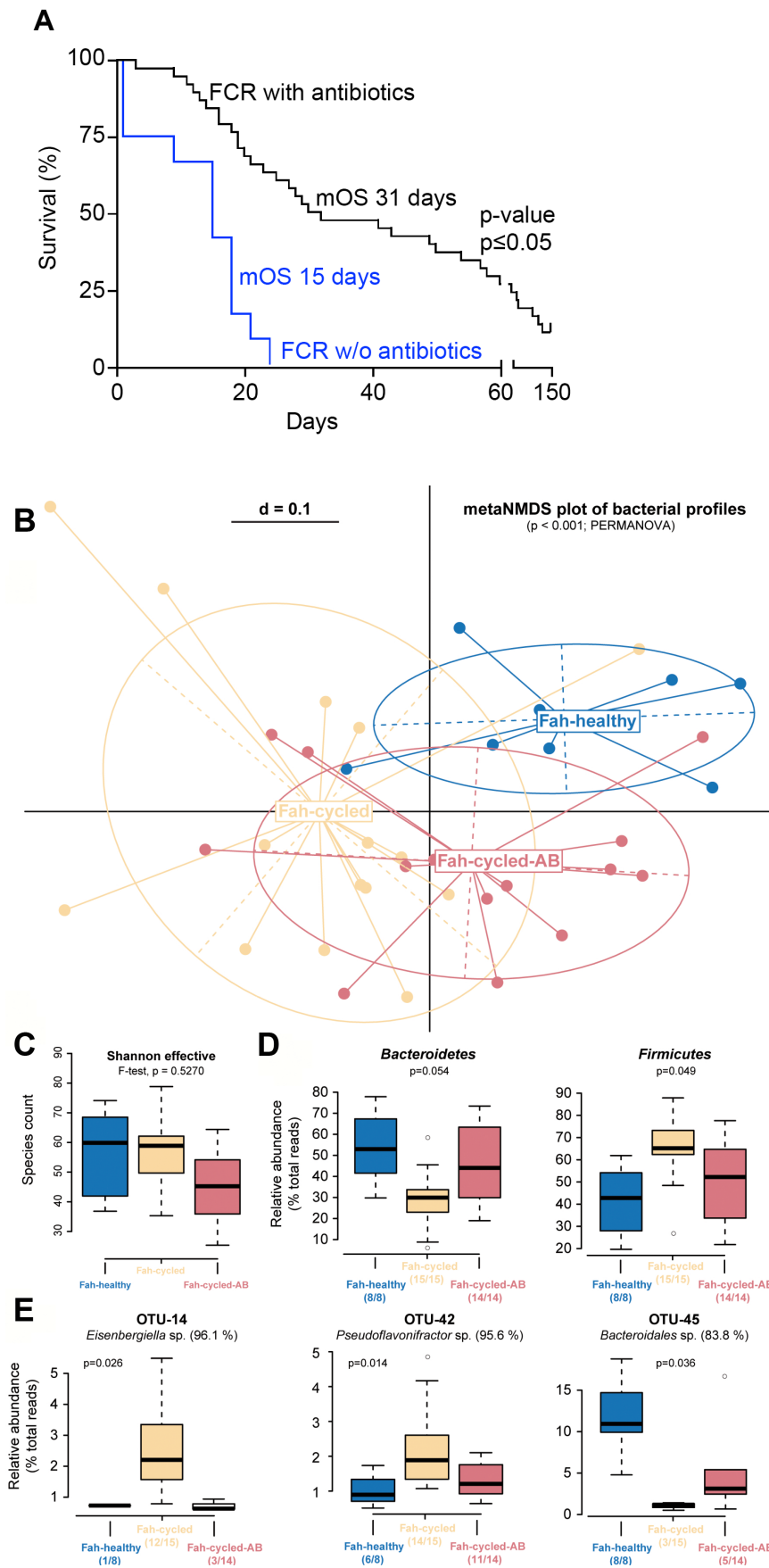


**Figure S5, related to Experimental Procedures:** (A) Kaplan-Meier plot showing the survival rates of FCR mice treated with and without antibiotics during NTBC cycling. Survival of cycled FCR mice was significantly improved under antibiotic treatment. (B-E) In order to track temporal changes on the quantity and composition of

the normal gut microbiota compensation, community fingerprinting approaches based on 16S rRNA gene sequencing from fecal DNA was performed in control *Fah*<sup>-/-</sup> mice on 100% NTBC and cycled *Fah*<sup>-/-</sup> mice with and without antibiotic treatment. Multidimensional analysis revealed marked inter-individual differences in the phylogenetic makeup of dominant fecal bacterial communities (B). Control *Fah*<sup>-/-</sup> mice on 100% NTBC (blue) formed a cluster that was distinct from cycled *Fah*<sup>-/-</sup> mice that underwent two NTBC withdrawals (yellow and red). Alpha-diversity was not significantly different between mouse groups, both at the level of taxa richness (data not shown) and Shannon effective counts (C), even after antibiotic treatment. (D) At the taxonomic level, control *Fah*<sup>-/-</sup> mice on 100% NTBC (blue) and cycled *Fah*<sup>-/-</sup> mice on antibiotics (red) showed increased relative abundances of sequences classified in the phylum *Bacteroidetes*, whereas cycled *Fah*<sup>-/-</sup> mice without antibiotics (yellow) were characterized by higher relative abundances of members of the phylum *Firmicutes*. These differences were mainly due to increased sequence counts of members of the family S24-7 within the *Bacteroidales* and an increase in the family *Lachnospiraceae*, respectively (data not shown). These changes in taxonomic composition were supported by only a few differences in the relative abundance of prevalent and dominant molecular species (E). Unknown members of the order *Bacteroidales* (e.g. OTU-45) were characteristic of control *Fah*<sup>-/-</sup> mice, whereas cycled *Fah*<sup>-/-</sup> mice were colonized by strains of genera within the Clostridiales. Boxplots show median and 25<sup>th</sup>/75<sup>th</sup> percentiles. The whiskers extend to the last data point within 1.5 x IQR (inter-quartile range).

## Supplemental Experimental Procedures

**Mouse treatments.** For suppression of T cell activation, experimental animals were subjected to cyclosporine A (CsA, 40µg/g) treatment once daily by oral gavage. Lymphotoxin-β receptor signaling was blocked by weekly i.p. injections of an anti-LTβR-Ig (or ctr.-Ig, 80µg/mouse). CD8 positive cells were depleted by i.p. injections of CD8 rat anti mouse antibody, clone RMCD8 (500 mg once, 200 mg every 5 days until sacrifice) (kindly provided by Christian Koenecke, Hannover Medical School, Germany). Mice were euthanized; blood and livers were collected after the second course of NTBC withdrawal and re-supplementation.

**Histology and Immunostaining.** Freshly dissected liver tissues were OCT-embedded or fixed in 3.7% formaldehyde, processed and paraffin-embedded. Three-micron sections were stained with hematoxylin and eosin (H&E) or processed for immunohistochemistry. Staining and quantification of histological slides (F4/80, A6, CD3, CD4, CD44v6) were performed as previously described (Vucur et al., 2013). Sirius red staining was performed following standard protocols. TUNEL assays were achieved according to the manufacturer's instructions (Roche & GE Healthcare). Detailed protocols are provided upon request. Five thousand hepatocytes were evaluated for Ki67 expression and the relative percentage of positively stained cells was calculated. Hepatocyte size was assessed based on b-Catenin staining (2000 hepatocytes per liver sample). Quantifications on histological sections were performed using ImageJ64 software. The H&E stained liver tissues were classified by a pathologist according to the Modified Ishak-Score in four categories for liver inflammation.

**Aminotransferase and Bilirubin Levels.** Blood was collected from the portal vein in lithium heparin tubes (LH1.3, Sarstedt, Germany) and processed according to the manufacturer's instructions. Aminotransferase activity and bilirubin levels were assessed using an Olympus AU 400 system (Beckman Coulter, Switzerland).

**In situ:** RNA in situ hybridization was performed using the RNAscope® 2.0 brown FFPE Assay (Advanced Cell Diagnostic) according to the manufacturer's protocol. Briefly, 2µm paraffin embedded tissue sections were baked for 1h in a dry oven at 60°C. After de-paraffinization and blocking of endogenous peroxidases, slides were cooked for 30 min before protease digestion. Murine Lymphotoxin-beta specific probes (Advanced Cell Diagnostic, CA, USA) were incubated for 2h at 40°C before signal amplification and detection and counterstaining with Hematoxylin I according to the assay protocol. Slides were mounted using EcoMount mounting medium (BioCare, Concord, CA) (Xia et al., 2016).

**Partial Hepatectomy and Hepatocyte Transplantation.** Partial hepatectomy (PH) was performed as previously described (Buitrago-Molina et al., 2009). Thirty-seven hours or one week after PH, mice were euthanized and livers were collected. For hepatocyte transplantation, hepatocytes from 6 weeks old C57Bl/6 mouse livers were isolated according to published protocols (Buitrago-Molina et al., 2009). One million hepatocytes were intrasplenically injected into *Fah*<sup>-/-</sup> and FCR mice. Subsequently, NTBC was withdrawn to induce liver repopulation.

**Adoptive Transfer of T Cells and CD8<sup>+</sup> cells.** CD3<sup>+</sup> T cells or CD8<sup>+</sup> cells were isolated from the spleen of *Fah*<sup>-/-</sup> mice and further enriched using a MACS cell separation system (Miltenyi Biotec, Germany). One million cells were adoptively transferred into FCR and FR mice by tail-vein injection. Subsequently, NTBC was withdrawn and re-supplemented as described above.

**Liver Progenitor Cell, Immune Cell Isolation and Flow Cytometry.** Liver progenitor cell (LPC) isolation and flow cytometry were performed as previously described (Dorrell et al., 2011). MIC1<sup>+</sup> and MIC1<sup>+</sup> CD133<sup>+</sup> cells within the CD45<sup>-</sup>, CD11b<sup>-</sup>, Ter119<sup>-</sup>, and CD31<sup>-</sup> cells were quantified by FACS. Livers were cleansed with a pre-warmed liver perfusion buffer. T, B and NK/NKT cell suspensions were generated by mechanical organ disruption through a 100µm nylon mesh (Sarstedt) and enriched using a 35% percoll gradient. For isolation of myeloid cells, perfused livers were enzymatically digested, disrupted by a gentleMACS™ Dissociator and enriched using a 40%/70% percoll gradient. Flow cytometry was performed on a BD FACS LSRII.

**Hepatic Hydroxyproline Content.** Liver tissue (30-40mg) was homogenized in 6N HCl and incubated at 110°C for 18 hours to allow hydrolysis. Hydrolysates were filtered and neutralized with 2,2% NaOH in citric acetate buffer. Neutralized hydrolysates were incubated with Chloramin-T solution, Perchloric Acid and Dimethylbenzaldehyde solution. Hydroxyproline levels were photometrically measured at 565nm.

**RNA Isolation.** Total RNA was extracted from non-tumor liver tissue using the MACHERY-NAGEL NucleoSpin RNA Isolation Kit.

**Microarray.** DNA Microarray Hybridization and Analysis was performed in the Microarray Core Facility of the Helmholtz Centre for Infectious Research (Braunschweig, Germany). RNA quality and integrity was assessed on an Agilent Technologies 2100 Bioanalyzer (Agilent Technologies; Waldbronn, Germany). 500ng of total RNA was subjected to Cy3-labelling using the one color Quick Amp Labeling protocol (Agilent Technologies; Waldbronn, Germany). Labeled cRNA was hybridized to a murine 4x44k Mouse V1 microarray (Agilent, Design ID: 014868) for 16h at 68°C and scanned using the Agilent DNA Microarray Scanner. Raw expression values were calculated using the software package Feature Extraction 10.5.1.1 (Agilent) and further analyzed using R package "Limma", log2 transformed and quantile normalized. For testing differential gene expression, normalized data sets were filtered for informative genes (showing at least expression values > log2(50) in more than two samples). Datasets were tested across all groups (ANOVA) or pairwise using linear models to assess differential expression in the

context of the multifactorial designed experiment. For statistical analysis and assessing differential expression, limma uses an empirical Bayes method to moderate the standard errors of the estimated log-fold changes.

**Gene Set Enrichment Analysis (GSEA).** GSEA is a computational method that determines whether a priori defined set of genes shows statistically significant, concordant differences between two biological states (e.g. phenotypes). GSEA was performed using function “gsePathway” from R package “ReactomePA” on datasets containing the differential expression data of two phenotypes. The selected genes sets were extracted from Reactome database. The minimal gene set size was 120 genes. The experimental dataset was permuted by 100 times to calculate the statistical significance. Gene sets with error corrected (Benjamini-Hochberg) adjP-Values less than 0.05 were collected (Yu et al., 2012).

**CGH arrays.** For genomic copy number analysis the Agilent SurePrint G3 Mouse CGH Microarray 4x180K (AMADID 027411) were used. Labelling, Hybridization, washing, scanning and data extraction was conducted according to the manufacturer’s protocol. Briefly, DNA was extracted from formalin-fixed paraffin embedded (FFPE) sections after macrodissection in order to enrich for tumour cells. Reference DNA was extracted from normal liver tissue of *Fah*<sup>-/-</sup> 100% NTBC control mice. Tumour and reference DNA was labelled and with Cy5-dCTP and Cy3-dCTP, respectively. Data were extracted after hybridisation, washing and scanning of slides and preprocessed as described in (Vucur et al., 2013) and (Wolf et al., 2014).

**Measurement of Chemokines and Growth Factors.** RNA was transcribed into cDNA with QuantiTect Reverse Transcription kit (Qiagen) according to the manufacturer’s instructions. RT<sup>2</sup> Profiler PCR Array for cytokines and chemokines (Qiagen) was achieved in agreement with producer’s suggestions. Expression of selected genes was validated by qRT-PCR performed on 7900 HT qRT-PCR system (Applied Biosystems) using the  $\Delta\Delta CT$  method. Relative mRNA levels of all target genes were normalized to two reference genes (HPRT and RHOT2).

**Immunoblotting.** Frozen liver tissue was subjected to homogenization (Ultra-Turrax, IKA, Germany) in cell lysis buffer (50mM HEPES, 50mM KCl, 50mM NaF, 5mM NaPPi, 1mM EDTA, 1mM EGTA, 5mM  $\beta$ -glycerolphosphate, 1mM DTT, 1mM vanadate, 1% (v/v) NP40) supplemented with a commercially available proteinase inhibitor cocktail (Complete, Roche) and centrifuged at 16,000g for 10 minutes. Protein concentration was measured using the Bio-Rad Protein Assay Dye Reagent. Proteins were separated via SDS-PAGE and blotted to activated-polyvinylidene difluoride membranes (Bio-Rad).

**Antibodies.** For immunohistochemistry, the following antibodies were utilized: CD11b (1:50) purchased from BD Pharmingen; APF (1:200) from BioCare Medical; F4/80 (1:120) BMA Biomedicals AG; cleaved caspase 3 (1:300) from Cell Signaling; a-sma (1:100) from Dako; CD44v6 (1:500) from eBioscience; FAH (1:500) from Genway; b-Catenin (1:50) from Santa Cruz; Ki67 (1:500) from Vector Laboratories; CD3 (1:250) from Zytomed; CD4-RMCD4.2 (1:100) and CD8-RMCD8.2 (1:100) kindly provided by Elmar Jäckel (MHH, Hannover); A6 (1:100) kindly provided by Valentina Factor (NIH, Washington DC). The following antibodies were utilized for FACS: NK1.1-PE (clone PK136) purchased from BD Pharmingen; B220-FICT (clone RA3-6B2), CD4-PerCP (clone RM4-5), CD62L-Pacific Blue (clone MEL-14), CD90.2-PE (clone 53-2.1), Ly6G-PE (clone 1A8) from Becton Dickinson; B220-PE (clone RA3-6B2), CD11c-BV605 (clone N418), CD4-PerCP (clone RM4-5), CD44-FICT (clone IM7), CD45-A700 (clone 30-F11), CD69-PerCP/Cy5.5 (clone H1.2F3), CD8-APC/Cy7 (clone 53-67) and F4/80-APC (clone BM8) from BioLegend; CD133-PE (clone 13A4), CD19-APC (clone MB19-1), CD25-PE (clone PC61.5), CD3-Pacific Blue (clone 17A2), CD31-FICT (clone 390), CD4-APC (clone GK1.5), CD8a-FICT (clone 53-6.7), NK1.1-PerCP/Cy5.5 (clone PK136) and Ter119-FITC (clone Ter-119) from eBioscience; MIC1 (clone 1C3) labeled with Cy5 Labeling Kit (PA35000) from Amersham was kindly provided by Craig Dorrell (OHSU, Portland). The following antibodies were utilized for Western Blotting: NQO1 (1:1000) purchased from abcam; HO-1 (1:2000) from ADI-SPA-896; actin (1:1000), cyclin D1 (1:500) and p21 (1:500) from Santa Cruz.



### Supplemental References

- van de Wiel, M. A., Kim, K. I., Vosse, S. J., van Wieringen, W. N., Wilting, S. M., and Ylstra, B. (2007). CGHcall: calling aberrations for array CGH tumor profiles. *Bioinformatics* 23, 892-894.
- van de Wiel, M. A., and Wieringen, W. N. (2007). CGHregions: dimension reduction for array CGH data with minimal information loss. *Cancer Inform* 3, 55-63.
- Vucur, M., Reisinger, F., Gautheron, J., Janssen, J., Roderburg, C., Cardenas, D. V., Kreggenwinkel, K., Koppe, C., Hammerich, L., Hakem, R., *et al.* (2013). RIP3 inhibits inflammatory hepatocarcinogenesis but promotes cholestasis by controlling caspase-8- and JNK-dependent compensatory cell proliferation. *Cell reports* 4, 776-790.
- Xia, Y., Stadler, D., Lucifora, J., Reisinger, F., Webb, D., Hosel, M., Michler, T., Wisskirchen, K., Cheng, X., Zhang, K., *et al.* (2016). Interferon-gamma and Tumor Necrosis Factor-alpha Produced by T Cells Reduce the HBV Persistence Form, cccDNA, Without Cytolysis. *Gastroenterology* 150, 194-205.
- Yu, G., Wang, L. G., Han, Y., and He, Q. Y. (2012). clusterProfiler: an R package for comparing biological themes among gene clusters. *OMICS* 16, 284-287.